Pergamon

SCIENCE DIRECT®

Bioorganic & Medicinal Chemistry 11 (2003) 3989–3996

BIOORGANIC & MEDICINAL CHEMISTRY

Computer-Aided Design of Non Sulphonyl COX-2 Inhibitors: An Improved Comparative Molecular Field Analysis Incorporating Additional Descriptors and Comparative Molecular Similarity Indices Analysis of 1,3-Diarylisoindole Derivatives

Asit K. Chakraborti* and R. Thilagavathi

Department of Medicinal Chemistry, National Institute of Pharmaceutical Education and Research (NIPER), Sector 67, S.A.S. Nagar, Punjab-160 062, India

Received 22 February 2003; revised 5 June 2003; accepted 7 June 2003

Abstract—A set of thirty five molecules of 1,3-diaryl-4,5,6,7-tetrahydro-2*H*-isoindoles endowed with selective COX-2 inhibitory activity was analyzed using comparative molecular field analysis (CoMFA) and comparative molecular similarity indices analysis (CoMSIA). Besides conventional steric and electrostatic fields, seven additional descriptors were incorporated to the CoMFA models. An improved CoMFA model ($r^2_{cv}=0.536$, $r^2_{conv}=0.968$, SEE = 0.222, $r^2_{pred}=0.6564$) was obtained by taking into account the CMR as additional descriptor. This analysis provided useful information regarding the pharmacophoric requirements for COX-2 inhibitory activity. FlexX was used to find out the binding orientation of this new class of 1,3-diaryl isoindoles in the active site of COX-2. The contour maps produced by improved CoMFA model was superimposed onto the active site revealing a good correlation between the contour maps and the active site residue interactions.

Introduction

Nonsteroidal anti-inflammatory drugs are widely used for the treatment of the symptoms of acute and chronic inflammatory disorders. Majority of the currently available NSAIDs inhibit both COX-1 and COX-2 exhibiting a selectivity in favour of COX-1.[1] The discovery and characterization[2,3] of COX-2 suggested that selective inhibition of this enzyme might avoid the side effects of currently available NSAIDs. This hypothesis has generated a great deal of interest in this field and various laboratories are aggressively pursuing this objective.

The first two lead compounds, Dup-697[4] and NS-398[5] (Fig. 1), that provided non ulcerogenic anti-inflammatory activity were reported by Dupont and Taisho, respectively. Successful outcome of the diaryl heterocycles, without any significant gastrointestinal injury, celecoxib and rofecoxib (Fig. 1) were marketed in 1998.

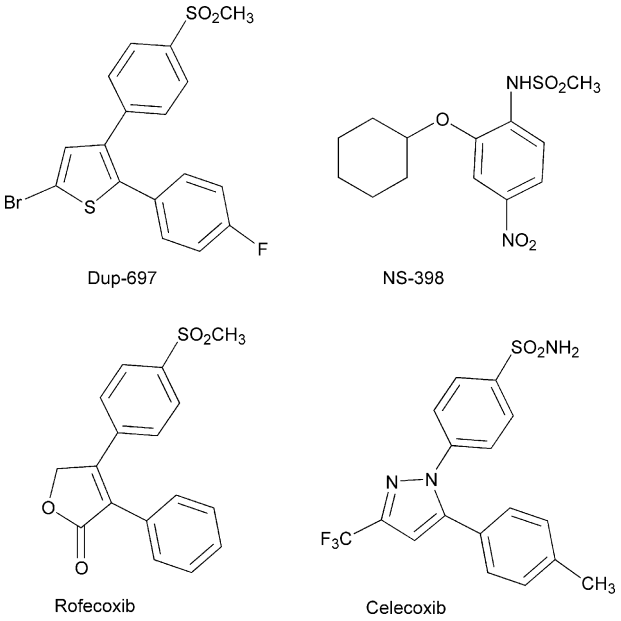

Figure 1. Structures of some selective COX-2 inhibitors.

*Corresponding author. Tel.: +91-172-214682; fax: +91-172-214692; e-mail: akchakraborti@niper.ac.in

0968-0896/03/$ - see front matter © 2003 Elsevier Ltd. All rights reserved.
doi:10.1016/S0968-0896(03)00404-8

Celecoxib and rofecoxib, respectively, exhibited a 375- and 1000-fold selectivity for COX-2 over COX-1 in vitro. Another most potent isoxazole sulfonamide, valdecoxib[6] is currently under phase III clinical trials. Parecoxib sodium,[7] a water soluble prodrug of valdecoxib is in clinical development as a parenteral formulation and has shown analgesic efficacy in patients after dental extraction. An oxazole derivative, JTE-522[8] and a combined COX-2/5-LOX inhibitors CI-1004[9] are under clinical investigation.

The 1,2-diaryl heterocyclic moiety having a sulphonyl group is a well recognised pharmacophore for selective COX-2 inhibitory activity.[10,11] Recently, 1,3-diaryl heterocyclic compounds[12,13] without sulphonyl group has been reported as selective COX-2 inhibitors. The aim of the present work was to obtain a 3-D QSAR model for 1,3-diaryl isoindoles devoid of sulfonyl group to delineate the various physicochemical properties attributing to the COX-2 inhibitory activity.

The comparative molecular field analysis (CoMFA)[14] and comparative molecular similarity indices analysis (CoMSIA)[15] are widely used as 3-D QSAR techniques. CoMFA relates the biological activity of a series of molecules with their steric and electrostatic fields sampled at grid points defining a large 3-D box around the molecule. The graphical representation (isocontour map) of CoMFA correlates the steric and electrostatic properties with the biological activity of the corresponding molecule in a data set. The basic principle of CoMSIA is the same as that of CoMFA, but includes some additional descriptors such as hydrophobicity, hydrogen bond donor and hydrogen bond acceptor. Although the 3-D descriptors are expected to contain information to give better prediction of biological activities than the 2-D descriptors, in some cases, 2-D descriptors appear to outperform the 3-D features.[16] Recent QSAR studies[17] carried out using 87 2-D descriptors and 798 3-D variables on a set of 5998 compounds emphasised the importance of both 2-D and 3-D descriptors and the incorporation of additional descriptors to CoMFA has been found to be useful in the refinement of 3-D QSAR models.[18,19] Therefore, we planned to use some additional descriptors as independent variables along with the CoMFA descriptors to obtain an improved 3-D QSAR model. As the active site of the cyclooxygenase is hydrophobic[20] in nature, we presumed that inclusion of the hydrophobicity parameter might play significant role in the model development. We also thought of adding HOMO energy as one of the additional descriptor as it was found in the literature[21,22] that there is a correlation between the HOMO energy and the cyclooxygenase inhibitory activity of NSAIDs. We also planned to use CoMSIA for establishing an improved model.

Results and Discussion

The COX-2 inhibitory activities reported from mouse resident peritoneal macrophages assay[12] were used for CoMFA studies.

Thirty five isoindole derivatives having different substituents on the pyrrole nitrogen and the aryl moieties were chosen for CoMFA studies. The training and test sets were constituted comprising with twenty nine and six molecules, respectively, encompassing a wide range ($pIC_{50} = 5.00–9.22$) of biological activity and substitution pattern (Table 1).

CoMFA and CoMSIA studies on 1,3-diaryl-4,5,6,7-tetrahydro-2*H*-isoindoles

The summary of the statistical results obtained for the CoMFA and CoMSIA studies are shown in Table 2. Out of the twenty nine molecules in the training set **4** and **31** were found to be outliers. The under prediction of **4** may be due to the presence of NH_2 group on the pyrrole nitrogen and the over prediction in case of **31** may be ascribed due to the presence of a pyridine instead of phenyl rings. Therefore, **4** and **31** were not considered for further analysis.

All the cross-validated results were analyzed by considering the fact that the value of r^2_{cv} above 0.3 indicates that the probability of chance correlation is less than 5%.[23] Among the two alignment methods (database, field-fit) tried, both the methods produced r^2_{cv} above 0.3 but the external predictions (test set) were found to be poor (r^2_{pred} 0.18) in case of the model obtained with field-fit aligned molecules. Since a good fit is not the only criterion in QSAR, the properties or the descriptors selected should work consistently for all the molecules in the series. Therefore, we used those molecules that are aligned using database method for further analysis. The model obtained using this method showed a good external predictivity (r^2_{pred} 0.65) but the r^2_{cv} was only 0.33 (Table 2).

In order to obtain an improved model, we adopted CoMSIA method. Thus, the incorporation of the hydrophobicity, hydrogen bond donor, and hydrogen bond acceptor parameters produced a model with a r^2_{cv} marginally better than that of CoMFA. However, the r^2_{conv} was found to be less. Hence, we planned to include some additional descriptors to improve the CoMFA model.

Incorporation of additional descriptors

In an effort to derive an improved model, CoMFA studies were performed with incorporation of seven additional descriptors such as the molecular volume, ClogP, CMR, HOMO, LUMO, dipole, and Coulson charge (on pyrrole nitrogen) and the results are summarised in Table 2. As the 1,3-diaryl heterocylclic compounds occupy more space in the active site of the enzyme (total volume 394 $Å^3$)[20] than the 1,2-diaryl heterocyclic compounds, we reasoned that molecular volume should have significant role (Fig. 3) in deriving the 3-D model. Thus, the incorporation of moleclar volume improved the r^2_{cv} from 0.331 to 0.560 amounting to a contribution of 13%. We further planned to find out the contribution of CMR in the model development as CMR represents the size and polarizability. Inclusion

Table 1. The structures and actual and predicted inhibitory activities (pIC_{50}) for the training and test set molecules of 1,3-diaryl 4,5,6,7-tetrahydro-2*H*-isoindoles

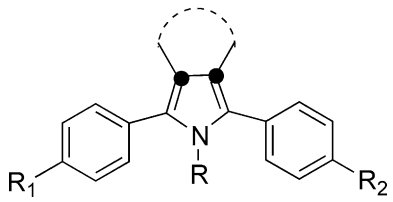

Compd	Ring	R	R_1	R_2	Actual pIC_{50}	Pred pIC_{50}	Residual	Set[a]
1		H	H	**H**	8.82	8.42	0.4	ts
2		H	H	H	8.48	8.44	0.44	tr
3		CH_3	H	H	6	6.11	−0.11	tr
4		NH_2	H	H	8.74	7.08	1.66	Outlier
5		$NHSO_2CH_3$	H	H	6.3	6.24	0.06	tr
6		CH_2COOH	H	H	7	6.4	0.6	ts
7		H	F	F	8.77	8.85	−0.08	tr
8		H	CH_3S	CH_3S	6.3	6.39	−0.09	tr
9		H	CH_3	CH_3	7.78	7.88	−0.11	tr
10		H	OCH_3	OCH_3	7.67	7.62	0.05	ts
11		H	Cl	Cl	8.3	8.22	0.08	tr
12		H	F	Imidazol-1-yl	7.38	7.37	0.01	tr
13		H	Imidazol-1-yl	Imidazol-1-yl	7	7.07	−0.07	tr
14		H	H	H	8.51	8.07	0.44	ts
15		H	H	**H**	7.84	8.08	−0.24	tr
16		CH_3	H	**H**	6	5.8	0.2	tr
17		H	H	**H**	9.15	8.51	0.64	tr
18		H	F	**F**	8.54	8.73	−0.19	tr

(*continued on next page*)

Table 1 (*continued*)

Compd	Ring	R	R_1	R_2	Actual pIC_{50}	Pred pIC_{50}	Residual	Set[a]
19	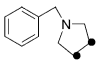	H	H	**H**	7	7.05	−0.05	tr
20		H	H	H	7	7.17	−0.17	tr
21		H	H	H	8.58	8.67	−0.09	tr
22		H	F	F	8.96	8.82	0.14	tr
23		H	F	F	8.35	8.5	−0.15	tr
24		H	F	CH_3SO_2	6.15	7.1	−0.95	ts
25		H	CH_3SO_2	CH_3SO_2	5	4.98	0.02	tr
26		H	H	H	8.79	8.72	0.07	tr
27		H	**F**	F	9.22	8.98	0.24	tr
28		H	H	H	7.45	7.86	−0.41	tr
29		H	4-F	4-F	7	6.84	0.16	tr
30		H	3-$NHCOCH_3$ 4-F	3-$NHCOCH_3$ 4-F	7	6.87	0.13	tr
31[b]		H	3-$NHCH_3$ —	3-$NHCH_3$ —	7	9.52	−2.52	Outlier
32	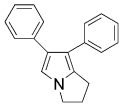				7.54	8.82	0.28	ts
33	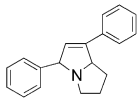				7.3	7.16	0.14	tr
34	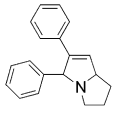				8	8.07	−0.07	tr
35	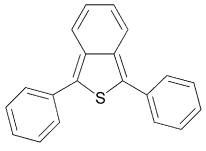				7.96	8.08	−0.12	tr

[a]tr = training set, ts = test set.
[b]Replacement of phenyl with pyridine.

Table 2. The summary of results of CoMFA-CoMSIA

	CoMFA alone		CoMSIA	CoMFA with additional descriptors					
	Db	FF	SEHDA	ClogP **1**	CMR **2**	MV **3**	HOMO **4**	1+2+3	1+2
r^2_{cv}	0.331	0.369	0.388	0.554	**0.536**	0.56	0.481	0.545	0.564
NOC	6	6	2	6	**6**	6	6	6	6
SEP	1.017	0.976	0.888	0.83	**0.846**	0.824	0.896	0.839	0.821
r^2_{conv}	0.964	0.991	0.647	0.968	**0.968**	0.963	0.961	0.972	0.973
SEE	0.235	0.115	0.675	0.22	**0.222**	0.24	0.246	0.208	0.204
F value	89.955	383.937	21.952	101.2	**101.556**	86.173	81.364	116.28	120.327
% Contr.									
Steric	44.2	39.9	4.3	44.9	**35.7**	36	38.8	34.2	34.7
Electrostaic	55.8	60.1	15.3	45.6	**50.4**	50.4	49.8	42	41.6
Hydro			9.6						
Donor			42.1						
Acceptor		18.3	28.6						
ClogP				9.5					10.6
CMR					**13.6**			10.5	13.1
Mol. Vol						13.6		11.6	
HOMO							11.4	1.7	
r^2_{pred}	0.6507	0.1834	0.597	0.534	**0.6564**	0.5998	0.5158	0.5748	0.57

Db = database alignment, FF = Fleld fit alignment, SEE = Standard error of estimate, SEP = Standard error of prediction, LOO = leave one out.

of CMR resulted in the improvement of the r^2_{cv} from 0.331 to 0.536 and prodcued good external predicitions ($r^2_{pred} = 0.6564$). However, compounds possessing CMR above 10 were found to be least active. The importance of ClogP could be realised in the improvement of the r^2_{cv} from 0.331 to 0.554 amounting to a contribution of 9.5%.

Among the electronic properties included, HOMO exhibited a r^2_{cv} of 0.481 and a contribution of 11%. Since HOMO offers a measure of the ease of loss of electron, under the present study an exact correlation of HOMO with biological activity was not possible. However, as the cyclooxygenase activity involves the oxidation of arachidonic acid the significance of the role of HOMO may be easily realised. Incorporation of LUMO field showed poor model and the addition of dipole and Coulson charge (on pyrrole nitrogen) did not improve the predictivity of the model.

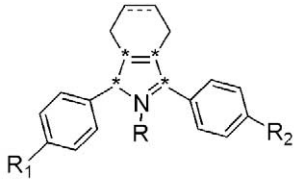

* used for atom based alignment

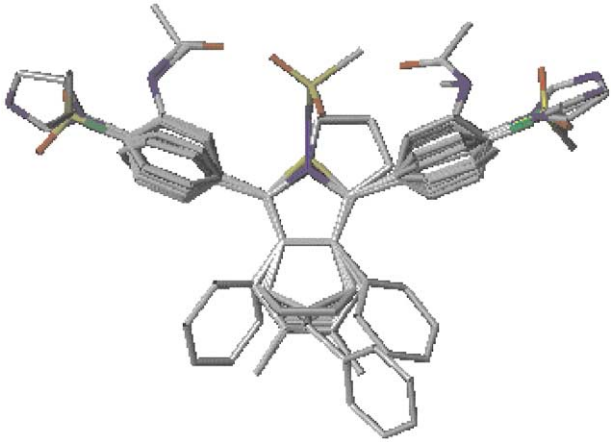

Figure 2. Alignment based on database method.

Among the various combinations tried, the inclusion of CMR and ClogP (Table 2) produced a model with a r^2_{cv} marginally better than that of CoMFA with either CMR and ClogP alone. But adding ClogP to CoMFA-CMR model decreased the external predictivity of that model. The incorporation of the electronic properties to the above model also did not provide any improved results. Garg et al.[24] reported a comparative QSAR study on various COX inhibitors in which the significant correlation between the molecular descriptors such as CMR, molecular volume, ClogP, HOMO and COX-2 inhibitory activity was observed. However, in some cases, combining many descriptors may affect the significance of individual property in the model development. The better predictivity with CMR (dealing with size and polarizability) and MV (dealing with size) compared to that of ClogP (dealing with lipophilicity)

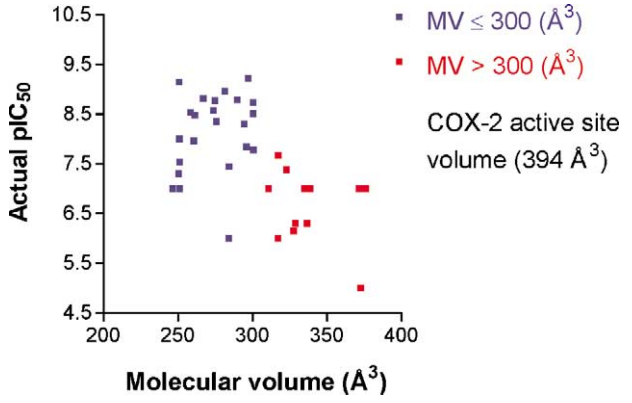

Figure 3. Molecular volume versus COX-2 inhibitory activity (pIC_{50}).

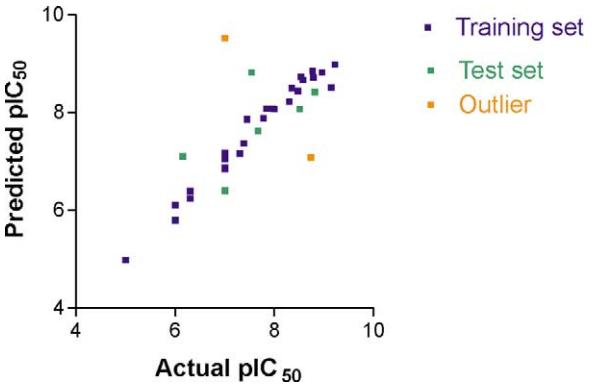

Figure 4. Plot between actual and predicted inhibitory activities (pIC_{50}) for all the molecules.

clearly indicates the importance of size (Fig. 3). Hence, the incorporation of ClogP either with CMR or with CMR and MV decreases the predictivity. Moreover, CoMFA calculates the steric component as non-bonded interactions (Van der Waals) between the substrate/ligand and the target enzyme/receptor whereas CMR calculates steric component by considering size (molecular weight) but also represents polarizability (Lorenz–Lorenz equation).[25] Since CMR represents polarizability apart from the size it can also serve as a measure of binding force between the polar portions of an enzyme/receptor and its substrate/ligand. Thus, CoMFA-CMR model was considered as final improved model with good internal and external predictions (Fig. 4). The 35, 50 and 13% contributions for the steric, electrostatic, and CMR respectively were observed for the above model. Further, we found that the CMR and ClogP of the potent inhibitors are close to the CMR and ClogP of arachidonic acid, a natural substrate for cyclooxygenase.

Analysis of CoMFA contour maps

For better understanding of the steric and electrostatic contour maps produced by CoMFA model, contour maps were superimposed on the active site of COX-2. The crystal structure of 1,2-diaryl heterocyclic compounds is available with enzyme, but the binding orientation of 1,3-diaryl heterocyclic compounds is not known. To obtain this information the most active molecule was docked into the active site of COX-2 using FlexX.[26] The contour maps produced by final CoMFA-CMR model were superimposed onto the active site and a good correlation between the contour maps and the active site residue interactions was observed. The big green contour (Fig. 5) on upper part of the pyrrole ring represents non-bonded interactions with the Val 349 and Arg 120, and Tyr 355 residues. The orientation of the two phenyl rings towards the red contours (Fig. 6) near the Ser 530, Ser 353, Ala 527, Ala 516 and Leu 352 residues indicates that an accumulation of positive charge on the phenyl rings should allow a favourable electrostatic interactions with these residues and accounts for the better activity of **27** bearing halogen substitution on the phenyl rings.

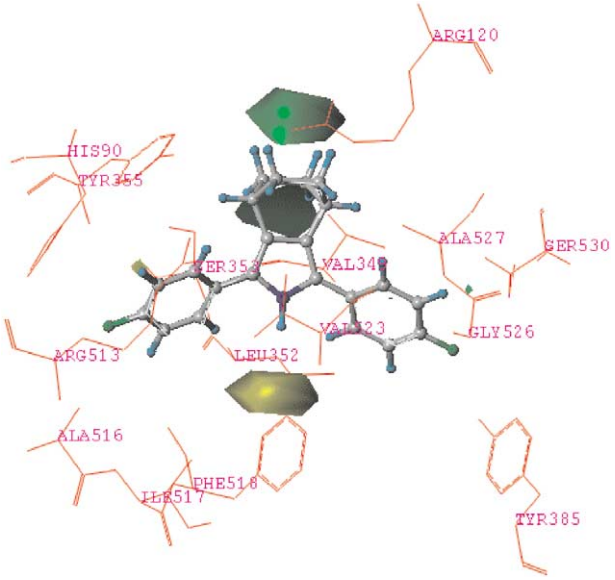

Figure 5. Steric contour maps produced by final CoMFA-CMR model was superimposed on COX-2 active site with molecule **27**.

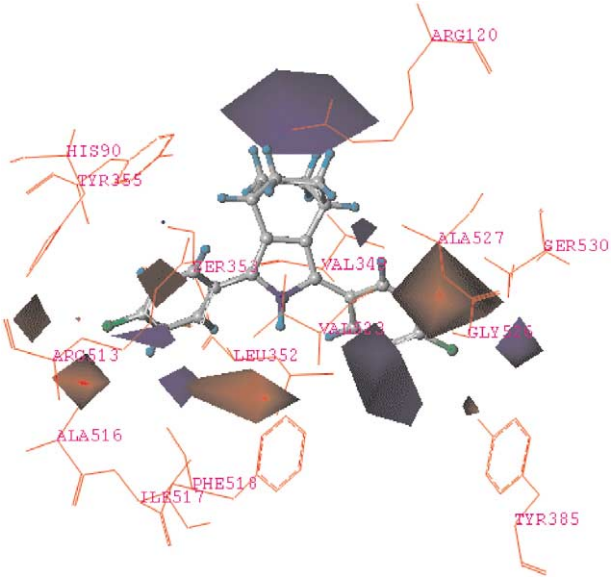

Figure 6. Electrostatic contour maps produced by final CoMFA-CMR model was superimposed on COX-2 active site with molecule **27**.

Conclusion

CoMFA and CoMSIA studies on thirty-five 1,3-diaryl 4,5,6,7-tetrahydro-2H-isoindoles have been performed. Among the various additional descriptors tried, CMR produced an improved CoMFA model.

The docking study enabled us to predict one of the possible conformations of 1,3-diaryl isoindole in the active site of cyclooxygenase-2. However, the exact orientation of the molecule in the active site may be confirmed through X-ray studies.

Finaly, the contour maps produced by CoMFA-CMR model were interpreted by superimposing them onto the

active site of COX-2 with the most active molecule. This information was found to be essential to understand the structure activity relationship of COX-2 inhibitory activity and the design of potential non-sulphonyl COX-2 inhibitors.

Experimental

Molecular modeling

The molecular modeling and 3-D QSAR studies were performed on a Silicon Graphics Octane 2 workstation using sybyl6.8.[27] Systematic conformational search was carried for the most active compound **27**. This was used as the template and the rest of the molecules have been modeled. Geometry optimization was performed using MMFF94[28] method including MMFF94 charges till the gradient convergence 0.05 kcal/mol was reached and these charges were used to calculate the electrostatic fields in the CoMFA analysis.

Alignment rules

One of the important steps in CoMFA and CoMSIA methods is the active conformation and alignment of molecules and the success of CoMFA and CoMSIA methods strongly depend on the relative positioning of the ligands in the fixed lattice, prior to the generation of the 3-D descriptors. We have performed two different alignments such as as is database alignment and the rigid field fit using QSAR≫Manage CoMFA≫ Alignments... command. The fragment used for the alignment is shown in Figure 2.

CoMFA interaction energy fields

The basic assumption of CoMFA is that the series of compounds having almost similar pharmacophore groups will interact and orient with its receptor/enzyme in similar fashion. To mimic such interactions, a 3-D grid box was put around the molecules taken for the study and CoMFA interaction fields were calculated at each lattice intersection of a regularly spaced grid of 2.0 Å by employing Lennard-Jones and Coulomb potentials. The CoMFA fields, depicting the steric and electrostatic interaction with an sp^3 carbon atom with +1.0 charge as the probe were calculated using Tripos force field. The steric and electrostatic fields were truncated at ±30.0 kcal/mol and the electrostatic fields were ignored at the points with maximal steric interactions.

PLS analysis

The regression analysis of CoMFA field energies was performed using the partial least squares (PLS) algorithm with the leave-one-out (LOO) method adopted for cross validation. The optimum number of components to be used in conventional analyses was chosen from the analysis with the highest cross validated r^2 value, and for component models with identical r^2 values, the model with the smallest standard error of prediction. The column filtering value (σ) was set to 2.0 for cross validated runs. Equal weightage was assigned to steric and electrostatic fields. Final analysis was carried out to calculate the conventional r^2 value using the optimum number of components.

CoMSIA interaction energy fields

The CoMSIA method is based on molecular similarity indices. Using a common probe atom, similarity indices were calculated for a data set of prealigned molecules at regularly spaced grid points. There is sudden rise in energy when the atoms of the molecules approach the probe atom. Therefore, the cut off value of >30 kcal/mol is included in CoMFA. This restriction may give some false interaction energy field values, which sometimes lead to error in the predictions. The gaussian type distance dependent functional forms used by CoMSIA method to calculate such properties overcome this problem. Similarity indices were calculated at all grid points inside and outside the molecules and evaluated in a PLS analysis following the usual CoMFA protocol.

Calculation of additional descriptors

The electronic descriptors such as dipole moment, HOMO and LUMO energies were calculated using MOPAC[29] inbuilt in SYBYL 6.8 with the key words 1scf, AM1, mmok, and the spatial descriptor, molecular volume was calculated using Alchemy2002.[30] The other properties such as CMR, ClogP were calculated using ChemDrawUltra6.0.[31] These descriptors were directly used in the PLS analysis.

Predictive r^2 value

To validate the derived models, biological activities of the test set molecules were predicted using models derived from training set. Predictive r^2 value was calculated using formula

$$r^2 \text{ predictive} = \frac{\text{SD-PRESS}}{\text{SD}}$$

where SD is the sum of squared deviation between the biological activities of the test set molecule and the mean activity of the training set molecules and PRESS is the sum of squared deviations between the actual and the predicted activities of the test set molecules.

Docking of the most active molecule

FlexX[26] was used to dock the most active molecule **27** into the active site. The crystal structure co-ordinates of 1CX2.pdb[31] were used for docking analysis. Active site of COX-2 was defined using the inhibitor SC-558,[31] and all amino acid residues within a 6.5 Å radius to any of the inhibitor atoms were specified and a core sub pocket was mentioned in order to obtain the appropriate bioactive conformation of the ligand within the active site. Hydrogens were supplied and the whole complex was refined in a stepwise manner using MMFF94[32] and the partial charges were calculated using MMFF94 method. The orientation of 1,3-diaryl ligand **27** in the

active site of COX-2 was used to superimpose the contours of CoMFA to find out the interaction with active site residue.

Supplementary material

The calculated additional descriptors for each molecule and the corresponding CoMFA results.

Acknowledgements

RT thanks Dr. Reddy's Research foundations Lab, Hyderabad, India for award of fellowship during the period of this work.

References and Notes

1. Sontag, S. J. *Drugs* **1986**, *32*, 445.
2. Fu, J. Y.; Masferrrer, J. L.; Sebert, K.; Raz, A.; Needleman, P. *J. Biol. Chem.* **1990**, *265*, 16737.
3. Xie, W.; Chipman, J. G.; Robertson, D. L.; Erikson, R. L.; Simmons, D. L. *Proc. Natl. Acad. Sci, U.S.A.* **1991**, *88*, 1692.
4. Gans, K. R.; Galbraith, W.; Roman, R. J.; Haber, S. B.; Kerr, J. S.; Schmidt, W. K.; Smith, C.; Hewews, W. E.; Ackerman, N. R. *J. Pharmacol. Exp. Ther.* **1990**, *254*, 180.
5. Futaki, N.; Takahashi, S.; Yokoyoyama, M.; Arai, I.; Higuchi, S.; Otomo, S. *Prostaglandins* **1994**, *47*, 55.
6. Talley, J. J.; Brown, D. L.; Carter, J. S.; Koboldt, C. M.; Masferrer, J. L.; Perkins, W. E.; Rogers, R. S.; Shaffer, A. F.; Zhang, Y. Y.; Zweifel, B. S.; Seibert, K. *J. Med. Chem.* **2000**, *43*, 775.
7. Talley, J. J.; Brown, D. L.; Carter, J. S.; Koboldt, C. M.; Masferrer, J. L.; Perkins, W. E.; Rogers, R. S.; Shaffer, A. F.; Zhang, Y. Y.; Zweifel, B. S.; Seibert, K. *J. Med. Chem.* **2000**, *43*, 1661.
8. Hashimoto, H.; Maeda, K.; Ozawa, K.; Haruta, J.-I.; Wakitani, K *Bioorg. Med. Chem. Lett.* **2002**, *12*, 65.
9. Song, Y.; Connor, D. T.; Doubleday, R.; Sorenson, R. J.; Sercel, A. D.; Unangst, P. C.; Roth, B. D.; Gilbertsen, R. B.; Chan, K.; Schrier, D. J.; Guglietta, A.; Bornemeier, D. A.; Dyer, R. D. *J. Med. Chem.* **1999**, *42*, 1151.
10. Desiraju, G. R.; Sarma, J. A. R. P.; Raveendra, D.; Gopalakrishnan, B.; Thilagavathi, R.; Sobhia, M. E.; Subramanya, H. S. *J. Phys. Org. Chem.* **2001**, *14*, 481.
11. Desiraju, G. R.; Gopalakrishnan, B.; Jetti, R. K. R.; Nagaraju, A.; Raveendra, D.; Sarma, J. A. R. P.; Sobhia, M. E.; Thilagavathi, R *J. Med. Chem.* **2002**, *45*, 4847.
12. Portevin, B.; Tordjman, C.; Pastoureau, P.; Bonnet, J.; Nanteuil, G. D. *J. Med. Chem.* **2000**, *43*, 4582.
13. Sui, Z.; Guan, J.; Ferro, M. P.; McCoy, K.; Wachter, M. P.; Murray, W. V.; Singer, M.; Steber, M.; Ritchie, D. M.; Argentieri, D. C. *Bioorg. Med. Chem. Lett.* **2000**, *10*, 601.
14. Cramer, I. I. I. R.D.; Patterson, D. E.; Bunce, J. D *J. Am. Chem. Soc.* **1988**, *110*, 5959.
15. Klebe, G.; Abraham, U.; Mietzner, T *J. Med. Chem.* **1994**, *37*, 4130.
16. Brown, R. D.; Martin, Y. C. *J. Chem. Inf. Comput. Sci.* **1996**, *36*, 572.
17. Oprea, T. I. *J. Braz. Chem. Soc.* **2002**, *13*, 811.
18. Waller, C. L.; Marshall, G. R. *J. Med. Chem.* **1993**, *36*, 2390.
19. Gokhale, V. M.; Kulkarni, V. M. *J. Med. Chem.* **1999**, *42*, 5348.
20. Luong, C.; Miller, A.; barnett, J.; Chow, J.; Ramesha, C.; Browner, M. F. *Nature Structural Biology* **1996**, *3*, 927.
21. Zoete, V.; Bailly, F.; Maglia, F.; Rougée, M.; Bensasson, R. V. *Free. Radic. Biol. Med.* **1999**, *26*, 1261.
22. Zoete, V.; Bailly, F.; Maglia, F.; Rougée, M.; Bensasson, R. V. *Free. Radic. Biol. Med.* **2000**, *28*, 1638.
23. Clark, M.; Cramer, R. D. *III., Jones, D.M., Patterson, D.E., Simeroth, P.E., Tetrahedron Comput. Methodol.* **1990**, *3*, 47.
24. Garg, R.; Kurup, A.; Mekapati, S. B.; Hansch, C. *Chem. Rev.* **2003**, *103*, 703.
25. Kubinyi, H. In Burger's Medicinal Chemistry and Drug Discovery. In: Wolff, M.E., Ed. Vol. 1 John Wiley & Sons, Inc. 1995 497–571.
26. Rarey, M.; Kramer, B.; Lengauer, T.; Kleb, G. *J. Mol. Biol.* **1996**, *261*, 470.
27. Tripos Associates, Inc., 1699 S. Hanley, St. Louis MI 63144, USA.
28. Halgren, T. *J. Am. Chem. Soc.* **1990**, *112*, 4710.
29. Merz, K. M.; Besler, B. H. *MOPAC*, Version 6.0 ESC; QCPE no. 455, with AM1 froce field parameters.
30. Cambridge Soft. Com, 100 Cambridge Park Drive, Cambridge, MA 02140, USA.
31. Abola, E. E.; Berstein, F. C.; Bryant, S. H.; Koetzle, T. F.; Weng, J. Protein Data Bank. In *Crystallographic Databases—Information Content, Software Systems, Scientific Applications*, Allen, F. H., Berjerhoff, G., Sievers, R. R., Eds.; Data Commission of the International Union of Crystallography: Bonn, 1987; pp 171.
32. Charifson, P. S.; Corkery, J. J.; Murcko, M. A.; Walters, W. P. *J. Med. Chem.* **1999**, *42*, 5100.